ERDC TN-24-1
JANUARY 2024

Scaled-Up Synthesis of Water-Retaining Alginate-Based Hydrogel

By Ashvin I. Fernando, Rebecca A. Crouch, Bobbi S. Stromer, Travis L. Thornell, Johanna N. Jernberg, and Erik M. Alberts

PURPOSE: Synthesis of a scaled-up version of a lithium-ion-based alginate/poly(acrylamide-*co*-stearyl methacrylate) [Li-alginate/P(AAm-*co*-SMA)] hydrogel with several optimizations for thermal signature investigations on various environmental substrates.

BACKGROUND: Hydrogels have been produced and explored in numerous applications, ranging from cell culturing to soft robotics (Liu et al. 2020). Hydrogels are a specific class of polymers that can retain a large amount of water—generally more than 20% of its dry weight (Pathak and Kumar 2017)—due to their unique three-dimensional network structure (Chamkouri 2021). The distinctive features of these network polymers depend on the nature and the arrangement of monomers, crosslinkers, ionic components, and the synthesis method (thermal, photochemical, etc.). The polymer chains in a hydrogel crosslink with each other chemically via covalent bond formation with monomers and crosslinking agents or physically via noncovalent interactions such as hydrogen bonding, crystallinity, hydrophobic interactions, and ionic interactions (Madduma-Bandarage and Madihally 2021).

Most hydrogel-based research described in recent literature has been at small scales to form thin films (Tokarev and Minko 2009). Therefore, the current research aimed to adapt the synthetic procedure of an existing desirable hydrogel formulation (Cui et al. 2019) to obtain a bulk-scale hydrogel that retains desirable properties and is much larger than most described in the literature.

MATERIALS: The following reagents were purchased and used as received:

sodium dodecyl sulfate (SDS) ACS (American Chemical Society) reagent, ≥99.0% (CAS# [Chemical Abstract service number] 151-21-3)
sodium chloride (NaCl) ReagentPlus®, ≥99% (CAS# 7647-14-5)
stearyl methacrylate (SMA), a mixture of stearyl and cetyl methacrylates that contains monomethyl ether hydroquinone (MEHQ) as an inhibitor (CAS# 32360-05-7)
acrylamide (AAm), suitable for electrophoresis, ≥99% (CAS# 79-06-1)
alginic acid sodium salt from brown algae (CAS# 9005-38-3)
N,N,N',N'–tetramethylethylenediamine (TEMED) ReagentPlus®, 99% (CAS# 110-18-9)
lithium chloride (LiCl) ACS reagent, ≥99% (CAS# 7447-41-8)
ammonium persulfate (APS) reagent grade, 98% (CAS# 7727-54-0)
Merck Millipore Milli-Q™ Reference Ultrapure Water

METHODOLOGY, RESULTS, AND DISCUSSION: The current work first set out to replicate the work of Cui et al. 2019 on a small scale to observe whether the reaction proceeded as described. Therefore, gels were formed in 10 cm diameter round molds. First, two solutions were prepared to create the gels: Solution A, a 7% (by mass) SDS, and Solution B, 0.5 M (molar) NaCl. Initially,

US Army Corps of Engineers®

Distribution Statement A. Approved for public release: distribution is unlimited.

these two solutions were mixed in equal parts. At this step, complete dissolution of the SDS was critical; to do that, the hybrid solution was heated at 68°C, which allowed the complete dissolution of SDS. It was also vital to ensure that no air bubbles remained in the SDS solution. Following mixing of Solutions A and B, 1% mol each of SMA and AAm was added. After the observation of complete dissolution, sodium alginate was added for a final mass percentage of 14% in each gel. Finally, 100 µl TEMED was added. The final mixture was loaded into molds and subjected to UV curing for 10 min to initiate photopolymerization, and the gels were stored undisturbed at room temperature for 24 hr. The obtained solid gel-like material was opaque and somewhat rigid and inflexible in structure.

Figure 1 shows that the specified order of the addition of chemicals is vital to form the necessary interactions while forming the hydrogel. During the polymer formation, AAm and SMA were added first; this allowed copolymerized PolyAAm-SMA. The formed polystearylmethacrylate (PSMA) was then able to penetrate inside the micelles formed by the SDS. This physical penetration into micelles allowed formation of physical crosslinking points. Then the incoming alginate could form physically interpenetrated polymer chains with polyacrylamide (PAAm) and aggregated PSMA.

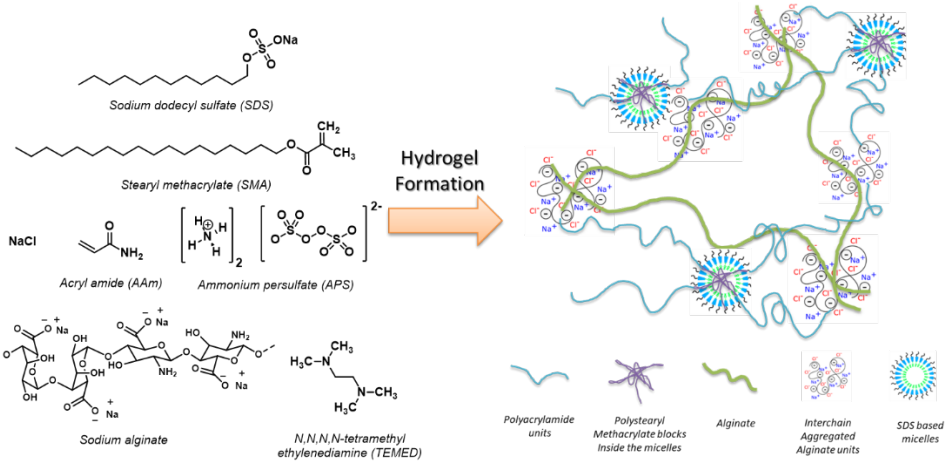

Figure 1. Chemicals used in the hydrogel formulations and chemical interactions that take place within the polymer matrix to form the desired hydrogel.

After the 24 hr curing process was complete, the gels were soaked in LiCl[1] solutions over a range of concentrations (0.1 M, 2 M, 4 M, and 8 M) for 5 hr for ion exchange. The gels soaked in 0.1 M and 2 M solutions became slightly transparent, very flexible, and contained more gel-like properties. The gels soaked in 4 M and 8 M solution developed a white color but retained the same elastic properties as the 0.1 M and 2 M soaked gels. Gels that were not soaked in LiCl solution formed NaCl crystals within the gel matrix due to faster evaporation rates of water from the hydrogel. Therefore, ion exchange with LiCl is essential to avoid NaCl crystal formations during drying of the hydrogel. Also, soaking in LiCl made the overall gel matrix more flexible. Furthermore, it is reported that the exchange of Na^+ ions to Li^+ ions makes the replacement from

1 For a full list of the spelled-out forms of the chemical elements used in this document, please refer to *US Government Publishing Office Style Manual*, 31st ed. (Washington, DC: US Government Publishing Office, 2016), 265, https://www.govinfo.gov/content/pkg/GPO-STYLEMANUAL-2016/pdf/GPO-STYLEMANUAL-2016.pdf.

larger ions to smaller ions, which allows the formation of much stronger binding interactions with carboxylate anions, thus increasing the overall strength of the gels (Sthoer et al. 2019). Figures 2 and 3 show the original and LiCl-soaked gels in detail.

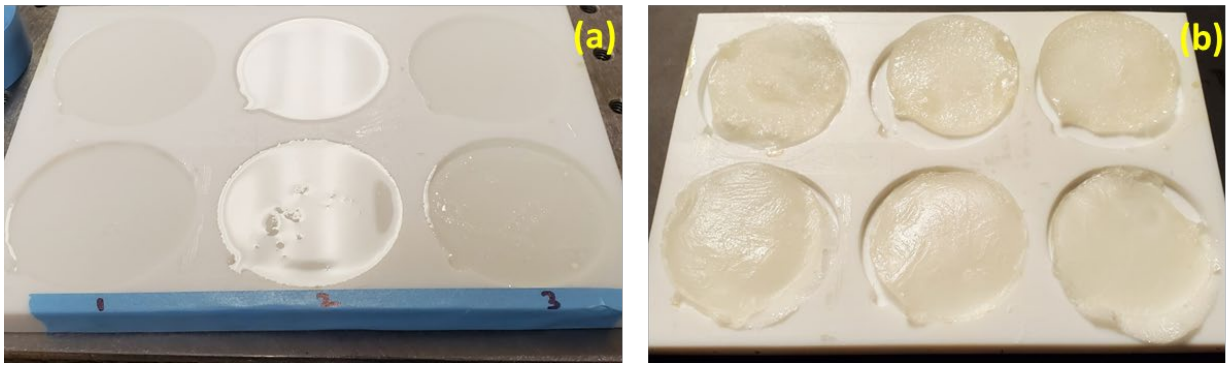

Figure 2. (*a*) Representation of the polymer solution immediately after addition into the mold (all mold sizes were uniform), and (*b*) the physical appearance of the formed gel before the LiCl soaking step.

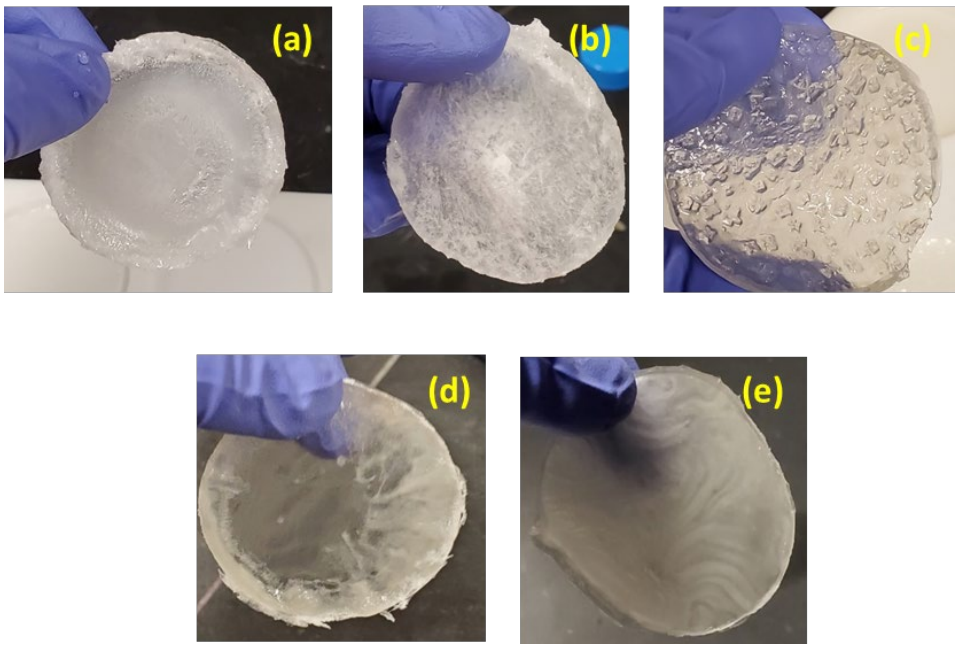

Figure 3. Hydrogel (*a*) with 0.5 M NaCl before LiCl soaking; (*b*) with 1 M NaCl before LiCl soaking; (*c*) without LiCl soaking steps, which shows NaCl crystallization within the hydrogel matrix; (*d*) soaked in 2 M LiCl solution, and (*e*) soaked in 4 M LiCl solution.

The results obtained from these preliminary experiments clarified the best method to form the desired hydrogel system. Figure 4 shows the complete methodology with the procedure of the scaled-up hydrogel formation setup.

During the scaled-up gel formulation processes, it was essential to ensure that all chemicals were properly mixed within the solution. Therefore, a mechanical stirrer, set at approximately 400 rpm, was used to ensure uniform mixing (Figure 4*a*). Also, as described in Scheme 1 in the figure, it was vital to obtain a clear, completely dissolved SDS/NaCl solution. To obtain a clear, fully

solvated solution, the solution was heated in a water bath at 68°C for 1 hr. During the addition of SMA and AAm, the solution remained white; but with the addition of sodium alginate, the solution changed into a more brownish-white color, and solution viscosity increased (Figure 5*b* and 5*c*).

Again, Figure 4 shows sodium alginate was added in small portions. Adding the alginate too quickly caused the solution to become extremely clumpy, and removing these clumps took several hours. Therefore, adding in the alginate in small amounts while stirring at max speed was necessary to avoid any formation of undissolved clumps. Large hydrogels were formed by pouring the final solution into large rectangular basins (Figure 6). Small areas of NaCl crystallization were again observed and tended to grow with time. These areas disappeared with addition of LiCl solution, which clearly demonstrated the exchange of larger sodium ions with much smaller lithium ions and formation of a more robust interaction with the gel (Figure 6*c*–6*f*). Figure 6*h* and 6*i* show stronger, more flexible gels resulted, even though gels were approximately 1 in. thick.

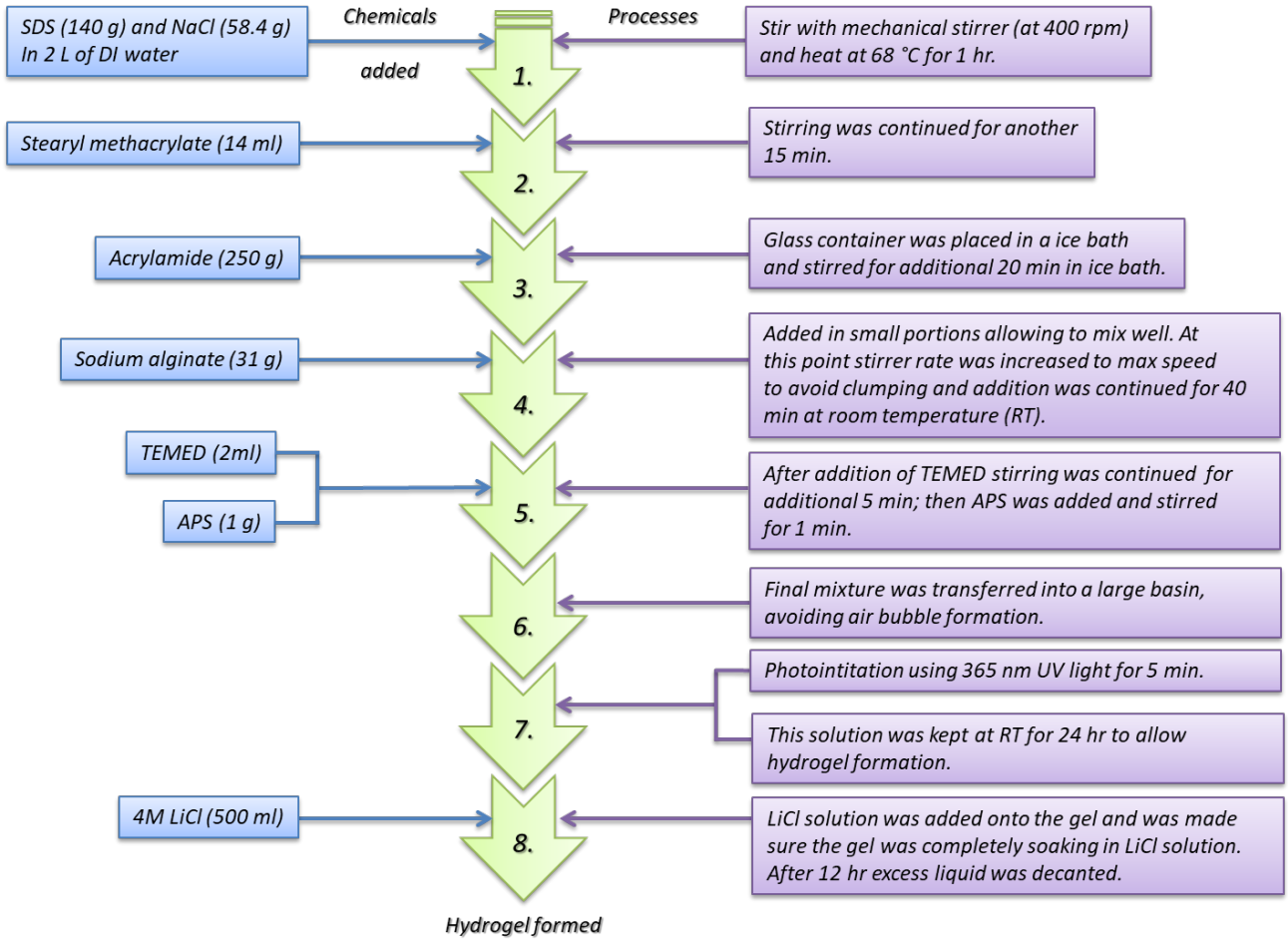

Figure 4. Complete scheme for the synthesis of scaled-up hydrogel formation: the *left* side represents the amounts of chemicals added in each step, and the *right* side represents the processes conducted after the addition of each chemical.

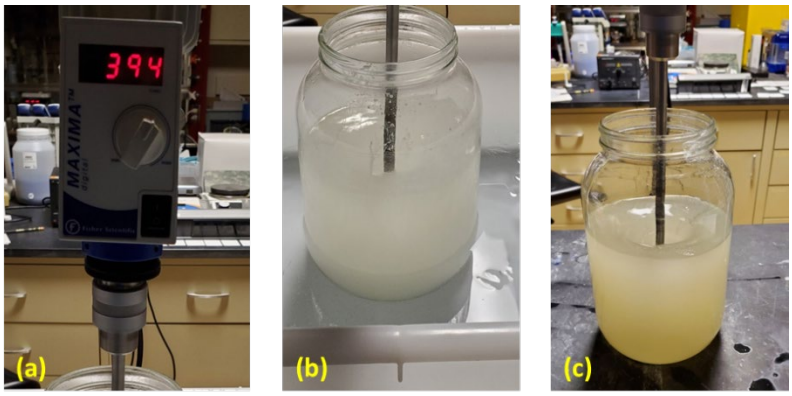

Figure 5. (*a*) Mechanical stirrer used during the mixing process of the solutions, (*b*) after addition of SMA/AAm, and (*c*) after addition of alginate.

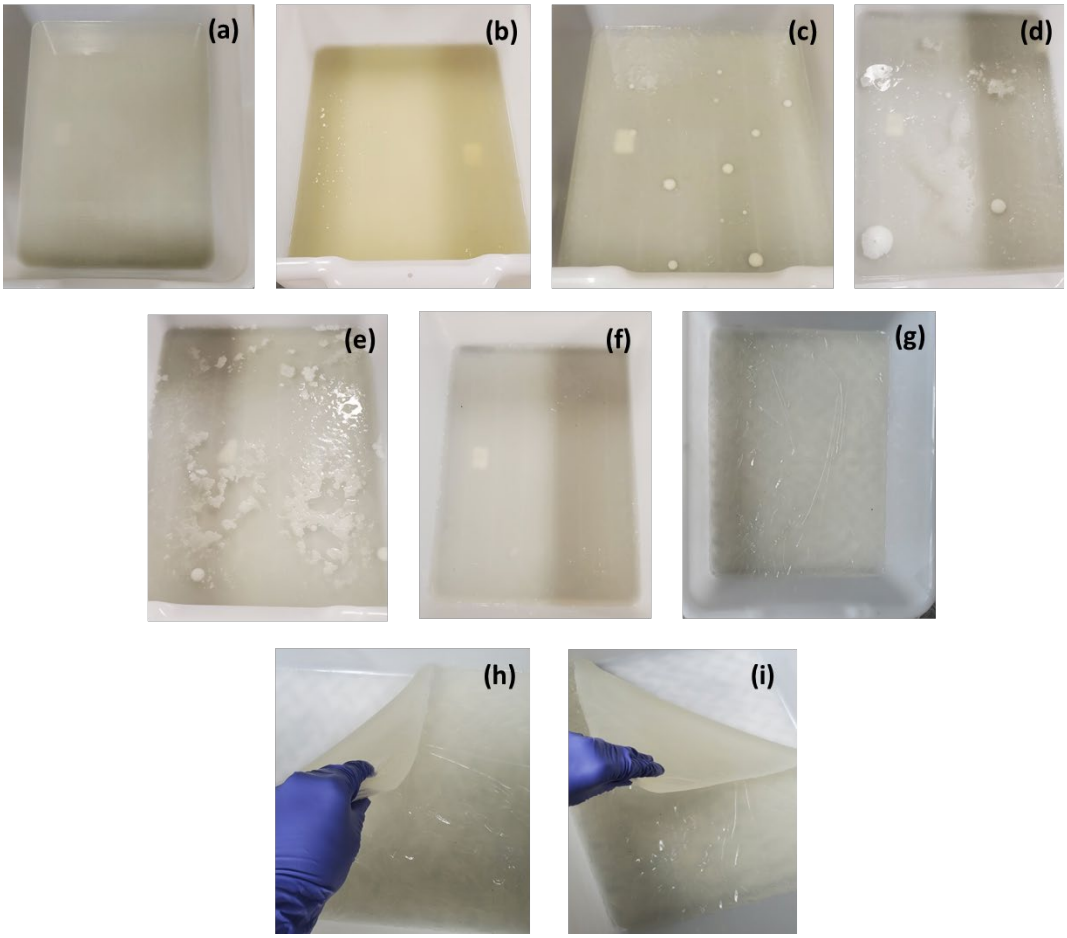

Figure 6. Gel (*a*) immediately after pouring into the large basin, (*b*) after 3 hr, (*c*) after 6 hr, (*d*) after 12 hr, (*e*) after 24 hr, (*f*) after addition of 4 M LiCl solution, (*g*) after storing for 7 days in refrigerator conditions, and (*h*) and (*i*) representation of the final hydrogel's flexibility.

CHARACTERIZATION AND ANALYSIS: After forming the bulk-scale hydrogels, small portions of gels were used for characterization via Fourier transform infrared spectroscopy (FT-

IR), scanning electron microscopy (SEM), energy dispersive X-ray (EDX), and thermograimetric analysis (TGA).

FT-IR Analysis: As Figure 6 shows, significant differences were observed between the synthesized bulk hydrogel and the starting materials. Compared to the FT-IR spectra of the starting materials, some peaks have disappeared for the bulk hydrogel. The peak assigned to the vibration of hydrogen of the functional group of alkene moiety (C=C–H) at 980 cm^{-1} is apparent for acrylamide monomer; however, this vibration band is not visible in the spectrum of the bulk hydrogels.

The two vibrational bands, which are visible in the acrylamide monomer at 1664.31 cm^{-1} and 1610.51 cm^{-1}, were no longer represented as two bands in the final bulk hydrogel and instead appear to be one broad single vibration band at around 1650 cm^{-1}, which shows the formation of polymeric materials. This is indicative of C=O vibrations, which suggests the targeted material had been successfully synthesized to form the bulk hydrogel with sufficient curing (Feng et al. 2018).

In the spectrum of sodium alginate, the broad peak around 3300 cm^{-1} was due to –OH stretching vibrations. The clear absorption peaks at approximately 1600 cm^{-1} and 1400 cm^{-1} were attributed to asymmetric and symmetric stretching vibrations of carboxylate groups of alginate, respectively (Figure 7). The peak at approximately 1030 cm^{-1} was assigned to the C–O stretching vibration of the polysaccharide structure present within the alginate (Ionita et al. 2013). Furthermore, in the spectra of bulk hydrogel, the characteristic peaks of both alginate and polyacrylamide could be observed, and no new distinct peaks were observed. Compared to the carboxylate group vibrations of alginate, these vibration peaks had significantly decreased in intensity within the bulk hydrogel, possibly due to the electrostatic interaction between metal ions and carboxyl anions or to the hydrogen bonding between alginate and polyacrylamide during the formation of the bulk hydrogel (Ionita et al. 2013). Another possibility is that the decrease in intensity for the bulk hydrogel could be the result of alginate chains being crosslinked to form a network through the strong electrostatic attraction between alginate chains and Na^{+} ions (Jing et al. 2020).

FT-IR signal intensities were further reduced after the exchange of sodium ions for lithium ions due to lithium ions' forming far superior electrostatic interaction within the alginate chains (Figure 8). However, as Figure 7 shows for pre-ion exchange, some residual peaks at approximately 2850 and 2950 cm^{-1}, likely indicative of –CH stretching from hydrocarbon chains (present in both SDS and SMA), were still observed. The intensities of these peaks were significantly decreased, possibly due to SDS and SMA's forming micelles. Within the micelles, crosslinking would result in the reduced intensity in the final bulk hydrogel.

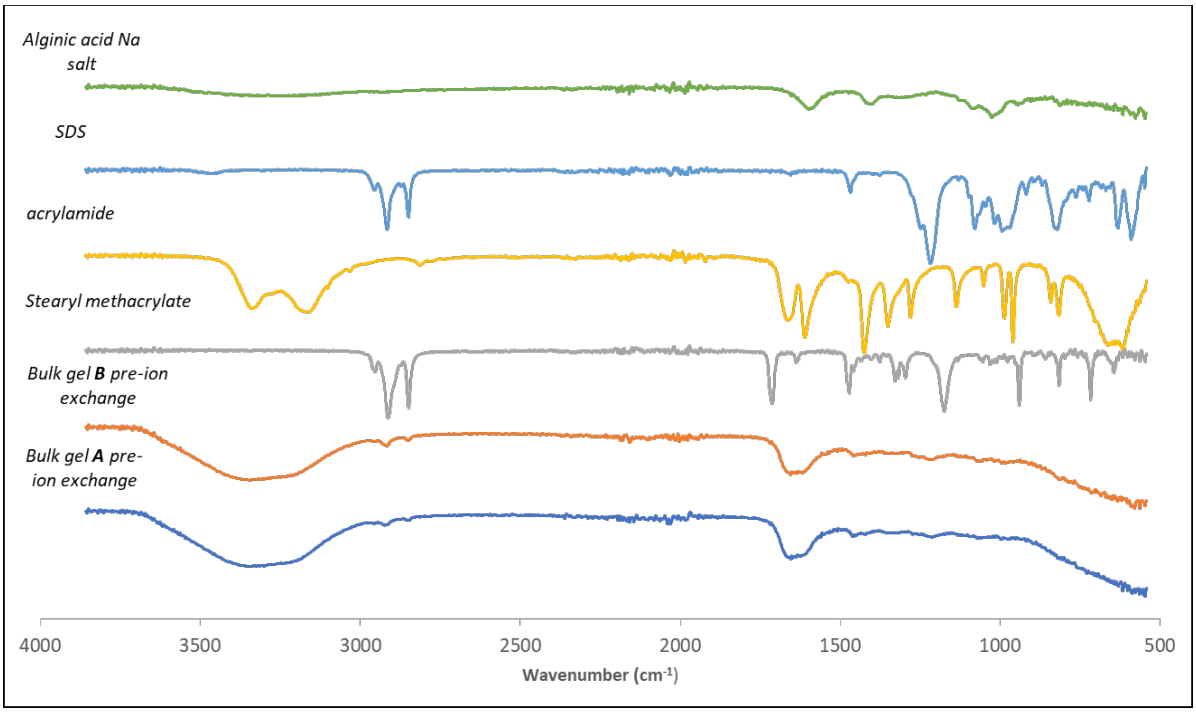

Figure 7. FT-IR spectra comparison between synthesized bulk gels and starting materials. Bulk A was the bulk gel synthesized without UV curing during the mixing stage, and Bulk B was the gel synthesized with UV curing during the mixing stage.

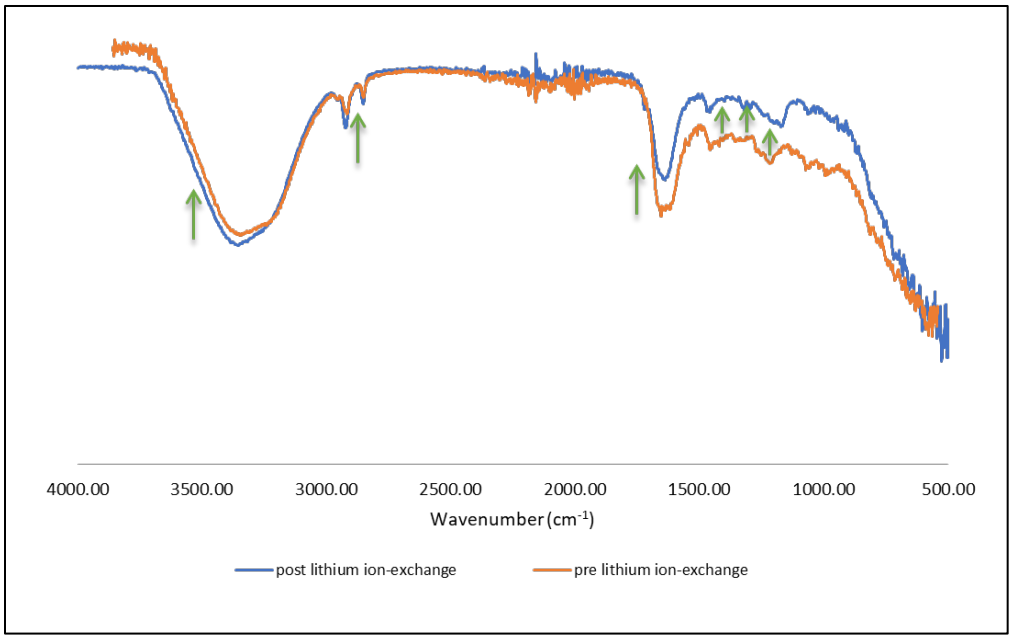

Figure 8. Stacked FT-IR spectra of the bulk hydrogel pre– and post–lithium ion exchange. *Arrows* represent areas of decreased signal intensity after lithium ion exchange.

SEM Analysis: Figure 9 shows SEM images were obtained before and after lithium ion exchanges. The gel specimens were prepared by freeze-drying for 24 hr, followed by cryogenic fracturing in liquid nitrogen. The morphology of the bulk hydrogel network deviated from a

homogeneous rough surface (Figure 9*a–c*) to a more porous structure with varying pore sizes (Figure 9*e* and 8*f*). As mentioned in previous literature, the reason for this phase is the separation of Li-alginate and P(AAm-*co*-SMA) networks (Cui et al. 2019) because the LiCl has a major effect on the hydrophilicity of alginate polyelectrolyte compared to NaCl, causing these porous structures to form due to increased phase separation. It is also noteworthy that there are regions of NaCl crystals within the gel matrix (Figures 8*d–f*), likely due to incomplete lithium ion exchange. If not enough time is given during the soaking process, unexchanged NaCl crystals may remain trapped within the gel network.

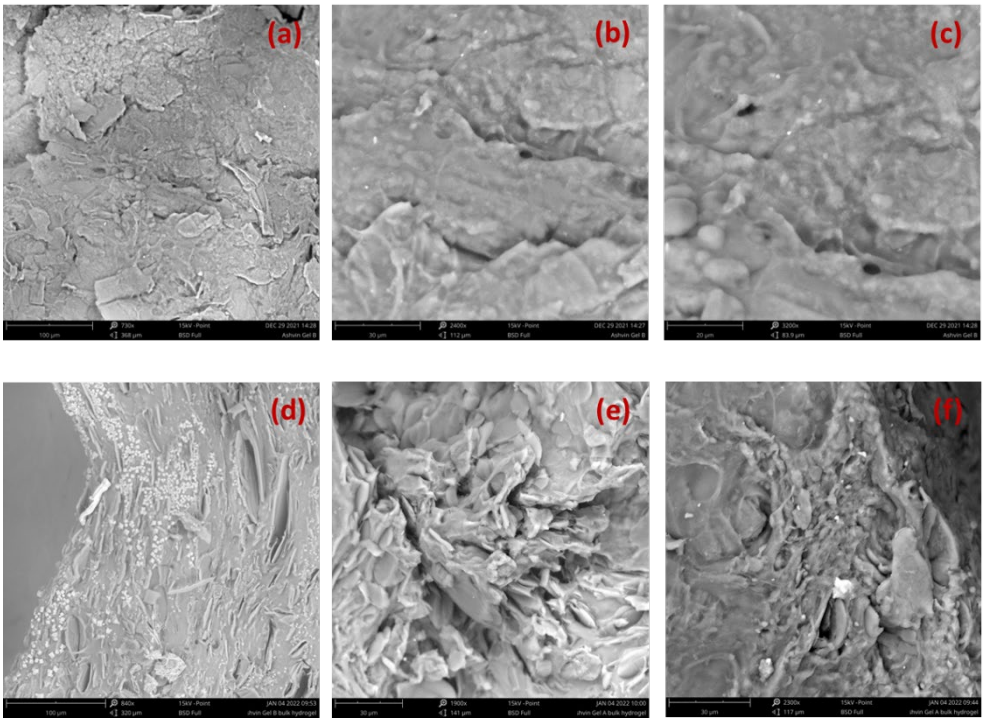

Figure 9. SEM images of bulk hydrogel before the lithium-ion exchange at (*a*) 100 µm, (*b*) 30 µm, and (*c*) 20 µm and after the lithium-ion exchange at (*d*) 100 µm, (*e*) 30 µm, and (*f*) 20 µm.

EDX Analysis: EDX analysis was performed before and after lithium ion exchanges, although Li^+ cannot be detected directly by EDX due to its low X-ray yield (Goldstein et al. 2018). Yet, the disappearance of characteristic peaks of sodium after the exchange occurred is evidence for successful ion exchange (Figure 10).

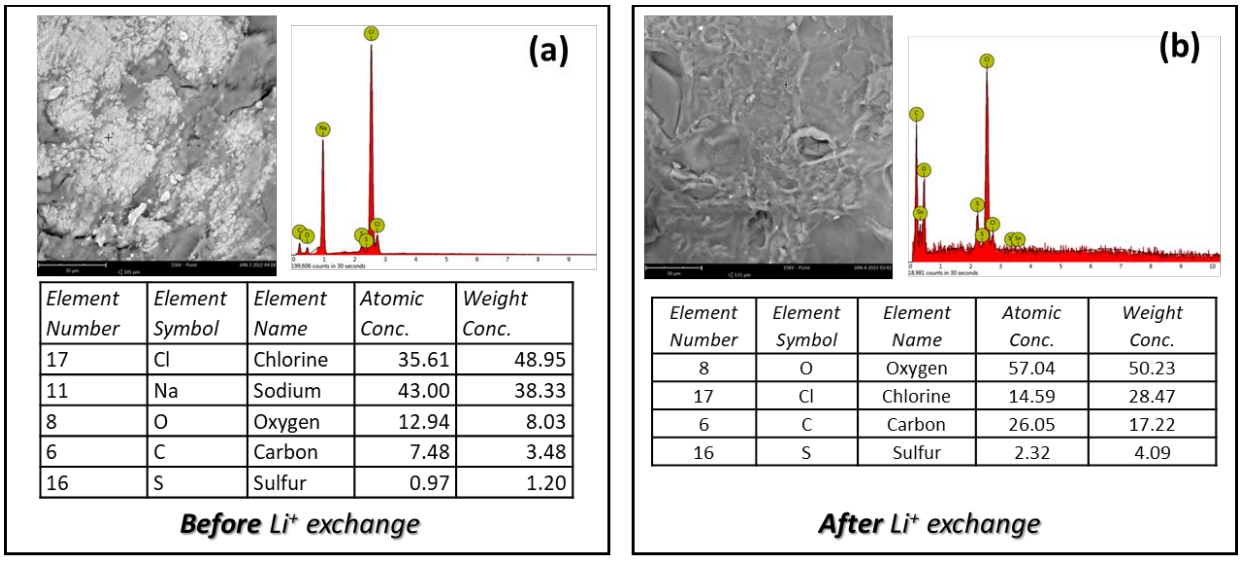

Element Number	Element Symbol	Element Name	Atomic Conc.	Weight Conc.
17	Cl	Chlorine	35.61	48.95
11	Na	Sodium	43.00	38.33
8	O	Oxygen	12.94	8.03
6	C	Carbon	7.48	3.48
16	S	Sulfur	0.97	1.20

***Before** Li⁺ exchange*

Element Number	Element Symbol	Element Name	Atomic Conc.	Weight Conc.
8	O	Oxygen	57.04	50.23
17	Cl	Chlorine	14.59	28.47
6	C	Carbon	26.05	17.22
16	S	Sulfur	2.32	4.09

***After** Li⁺ exchange*

Figure 10. EDX spectra in the location as shown in the image and the related elemental composition (*a*) before and (*b*) after lithium ion exchange.

TGA Data: For TGA studies, samples were collected before and after Li^+ exchange to observe the role of Li^+ in retaining water. As seen in Figure 11*a*, the weight loss at 150°C is greatly affected by incorporation of Li^+. For hydrogels before Li^+ exchange, the swollen hydrogels exhibited high levels of weight loss (approximately 70%) from the removal of water from gel networks. After Li^+ exchange, the hydrogels lost only ~15% weight in this region. This indicated an increase in the water retention of these hydrogel networks with Li^+ exchange.

This was observed for the gels both with UV (Figure 11*a*) or without UV (Figure 11*b*) crosslinking. Both gels behaved similarly after the Li^+ exchange (Table 1). As temperature increased across the tested range up to 800°C, other weight loss events were observed in the TGA-derivative plot in Figure 10*b* (UV cured). For these regions, the weight loss could possibly be attributed to polymer hydrogel network thermal degradation. The hydrogels after Li^+ exchange indicated higher degradation at regions of 150°C–240°C and 240°C–450°C compared to hydrogels before Li^+ exchange. This can be potentially attributed to the swelling degree of the networks from salt screening effects.

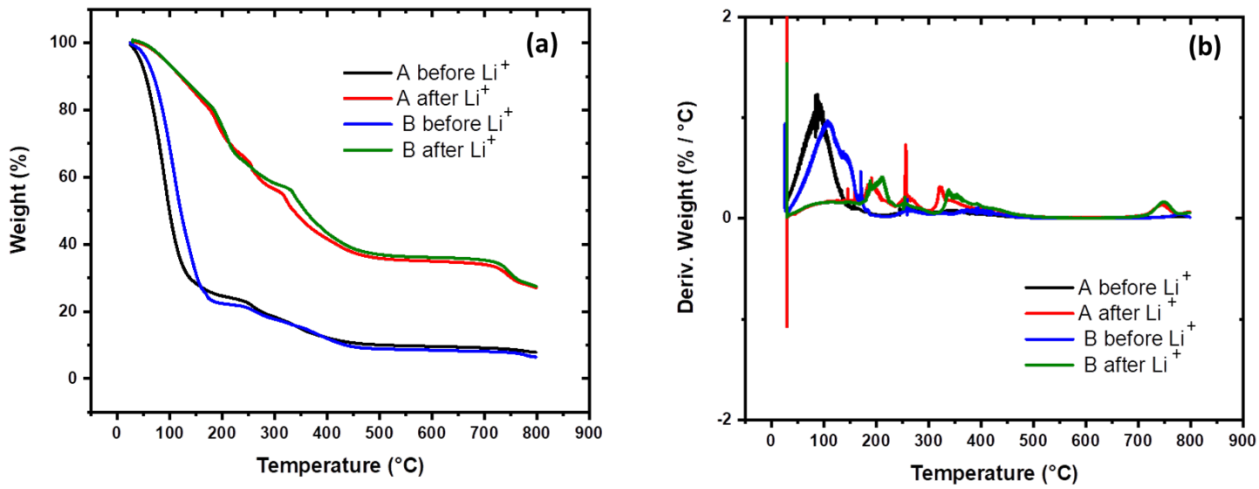

Figure 11. TGA data for hydrogels before and after lithium exchange.

Table 1. Percentage weight loss before and after lithium ion exchanges: (*A*) bulk hydrogel with UV curing and (*B*) bulk hydrogel without UV curing.

Sample	Weight Change (%)		
	30°C–50°C	150°C–240°C	240°C–450°C
A before Li^+ exchange	70.24%	5.25%	12.5%
A after Li^+ exchange	15.47%	28.74%	28.74%
B before Li^+ exchange	68.03%	9.86%	12.02%
B after Li^+ exchange	15.15%	20.7%	26.17%

BEHAVIOR IN ENVIRONMENT: Figure 12 compares the alginate-LiCl hydrogel (*bottom*) and a simple agar hydrogel (*top*). The red box indicates an area on the agar gel that began rupture immediately upon exposure to environmental conditions due to mechanical and thermal instability. Meanwhile, the synthesized bulk hydrogel remained without mechanical breakage, thermally induced loss (melting and evaporation), or dissolution (local precipitation events) even after several weeks. The agar hydrogel showed shrinkage and cracking after a few days, while the synthesized bulk alginate-LiCl hydrogel experienced negligible shrinkage even after several weeks and continued to rehydrate upon local precipitation in Vicksburg, Mississippi, in June 2021. Thermal signature investigations are reported separately.[2]

[2] Report currently in preparation.

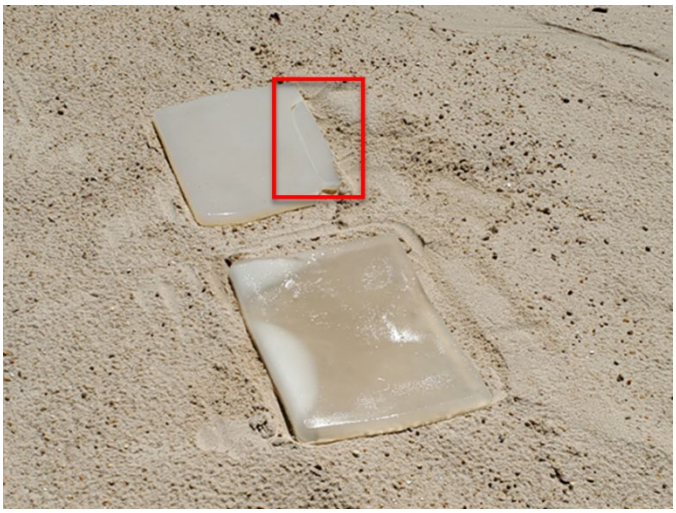

Figure 12. Bulk hydrogel used in field studies to observe thermal signatures of gel matrices versus control: simple agar hydrogel with *red box* showing small area of mechanical instability immediately upon environmental exposure (*top*) and clear bulk alginate-LiCl hydrogel reported herein (*bottom*).

SUMMARY: Hydrogel synthesis was scaled up efficiently. No loss of desirable properties was observed. The scaled-up process allowed production of large quantities of hydrogel. The bulk hydrogel was characterized using FT-IR, SEM, EDX, and TGA. FT-IR showed that there were significant differences between the starting materials and the hydrogel, confirming the formation of hydrogel structure. Future studies will focus on conducting a series of rheology studies and swelling studies to further understand the mechanical properties of this synthesized bulk hydrogel. In parallel, investigations will continue toward developing the hydrogels into materials with desireable thermal and spectroscopy properties. Additionally, a green-chemistry basis synthesis will also be pursued.

AUTHOR CONTRIBUTIONS: This technical note was prepared with equal contributions by Dr. P. U. Ashvin I. Fernando, senior scientist, Bennett Aerospace Inc.; Dr. Rebecca A. Crouch, research chemist, Environmental Laboratory, US Army Engineer Research and Development Center (ERDC); and Bobbi S. Stromer, formerly research chemist, Environmental Laboratory, ERDC. Dr. Travis L. Thornell, research physical scientist, ERDC Geotechnical and Structures Laboratory, assisted in obtaining and interpreting TGA data. Dr. Erik M. Alberts, of SIMETRI, Inc. assisted in obtaining and interpreting SEM data. Johanna N. Jernberg, Oak Ridge Institute for Science and Education (ORISE), assisted with hydrogel synthesis. Permission to publish was granted by the director, Geotechnical and Structures Laboratory.

POINTS OF CONTACT: For additional information, contact Dr. Rebecca Crouch (rebecca.a.crouch@erdc.dren.mil, Dr. Ashvin Fernando (payagala.a.fernando@erdc.dren.mil), and Dr. Travis Thornell (travis.l.thornell@erdc.dren.mil). This technical note should be cited as follows:

Fernando, A. I., R. A. Crouch, B. S. Stromer, T. L. Thornell, J. N. Jernberg, and E. M. Alberts. 2023. *Scaled-Up Synthesis of Water-Retaining Alginate-Based Hydrogel*. ERDC TN-24-1. Vicksburg, MS: US Army Engineer Research and Development Center, Geotechnical and Structure Laboratory. http://dx.doi.org/10.21079/11681/48032.

REFERENCES

Chamkouri, Hossein. 2021. "A Review of Hydrogels, Their Properties and Applications in Medicine." *American Journal of Biomedical Science & Research* 11 (6): 485–93. https://doi.org/10.34297/ajbsr.2021.11.001682.

Cui, Xiao Feng, Wen Jiang Zheng, Wei Zou, Xing Yong Liu, Hu Yang, Jie Yan, and Yang Gao. 2019. "Water-Retaining, Tough and Self-Healing Hydrogels and Their Uses as Fire-Resistant Materials." *Polymer Chemistry* 10 (37): 5151–58. https://doi.org/10.1039/c9py01015g.

Feng, Lijuan, Huaiyu Yang, Xiqing Dong, Haibo Lei, and Di Chen. 2018. "PH-Sensitive Polymeric Particles as Smart Carriers for Rebar Inhibitors Delivery in Alkaline Condition." *Journal of Applied Polymer Science* 135 (8): 45886. https://doi.org/10.1002/APP.45886.

Goldstein, Joseph I., Dale E. Newbury, Joseph R. Michael, Nicholas W. M. Ritchie, John Henry J. Scott, and David C. Joy. 2018. "Scanning Electron Microscope (SEM) Instrumentation." In *Scanning Electron Microscopy and X-Ray Microanalysis*, 65–91. https://doi.org/10.1007/978-1-4939-6676-9_5.

Ionita, Mariana, Madalina Andreea Pandele, and Horia Iovu. 2013. "Sodium Alginate/Graphene Oxide Composite Films with Enhanced Thermal and Mechanical Properties." *Carbohydrate Polymers* 94 (1): 339–44. https://doi.org/10.1016/J.CARBPOL.2013.01.065.

Jing, Zhanxin, Xiangyi Dai, Xueying Xian, Xiaomei Du, Mingneng Liao, Pengzhi Hong, and Yong Li. 2020. "Tough, Stretchable and Compressive Alginate-Based Hydrogels Achieved by Non-Covalent Interactions." *RSC Advances* 10 (40): 23592–606. https://doi.org/10.1039/D0RA03733H.

Liu, Xinyue, Ji Liu, Shaoting Lin, and Xuanhe Zhao. 2020. "Hydrogel Machines." *Materials Today* 36 (June): 102–24. https://doi.org/10.1016/j.mattod.2019.12.026.

Madduma-Bandarage, Ujith S. K., and Sundararajan V. Madihally. 2021. "Synthetic Hydrogels: Synthesis, Novel Trends, and Applications." *Journal of Applied Polymer Science* 138 (19). https://doi.org/10.1002/app.50376.

Pathak, Vinay Mohan, and Navneet Kumar. 2017. "Dataset on the Superabsorbent Hydrogel Synthesis with SiO2 Nanoparticle and Role in Water Restoration Capability of Agriculture Soil." *Data in Brief* 13: 291–94. https://doi.org/10.1016/j.dib.2017.05.046.

Sthoer, Adrien, Jana Hladílková, Mikael Lund, and Eric Tyrode. 2019. "Molecular Insight into Carboxylic Acid-Alkali Metal Cations Interactions: Reversed Affinities and Ion-Pair Formation Revealed by Non-Linear Optics and Simulations." *Physical Chemistry Chemical Physics* 21 (21): 11329–44. https://doi.org/10.1039/c9cp00398c.

Tokarev, Ihor, and Sergiy Minko. 2009. "Stimuli-Responsive Hydrogel Thin Films." *Soft Matter* 5 (3): 511–24. https://doi.org/10.1039/b813827c.

NOTE: *The contents of this technical note are not to be used for advertising, publication, or promotional purposes. Citation of trade names does not constitute an official endorsement or approval of the use of such products.*